Icarus 245 (2015) 367–378

Contents lists available at ScienceDirect

Icarus

journal homepage: www.elsevier.com/locate/icarus

Micrometer-scale U–Pb age domains in eucrite zircons, impact re-setting, and the thermal history of the HED parent body

M.D. Hopkins [a,e], S.J. Mojzsis [a,b,c,e,*], W.F. Bottke [d,e], O. Abramov [e,f]

[a] Department of Geological Sciences, University of Colorado, UCB 399, 2200 Colorado Avenue, Boulder, CO 80309-0399, USA
[b] Laboratoire de Géologie de Lyon, Ecole Normale Supérieure de Lyon & Université Claude Bernard Lyon 1, CNRS UMR 5276, 2 rue Raphaël DuBois, Bât. Geode 3e, 69622 Villeurbanne, France
[c] Institute for Geological and Geochemical Research, RCAES, Hungarian Academy of Sciences, Budaörsi ut 45, Budapest H-1112, Hungary
[d] Department of Space Studies, Southwest Research Institute, 1050 Walnut Street, Suite 400, Boulder, CO 80302, USA
[e] Center for Lunar Origin and Evolution (CLOE), NASA Lunar Science Institute, USA
[f] United States Geological Survey, Astrogeology Research Program, 2255 N. Gemini Dr., Flagstaff, AZ 86001, USA

ARTICLE INFO

Article history:
Received 5 June 2014
Revised 12 August 2014
Accepted 15 August 2014
Available online 23 August 2014

Keywords:
Asteroid Vesta
Geological processes
Asteroids dynamics
Cosmochemistry

ABSTRACT

Meteoritic zircons are rare, but some are documented to occur in asteroidal meteorites, including those of the howardite–eucrite–diogenite (HED) achondrite clan (Rubin, A. [1997]. Meteorit. Planet. Sci. 32, 231–247). The HEDs are widely considered to originate from the Asteroid 4 Vesta. Vesta and the other large main belt asteroids record an early bombardment history. To explore this record, we describe sub-micrometer distributions of trace elements (U, Th) and $^{235,238}U$–$^{207,206}Pb$ ages from four zircons (>7–40 μm ∅) separated from bulk samples of the brecciated eucrite Millbillillie. Ultra-high resolution (~100 nm) ion microprobe depth profiles reveal different zircon age domains correlative to mineral chemistry and to possible impact scenarios. Our new U–Pb zircon geochronology shows that Vesta's crust solidified within a few million years of Solar System formation (4561 ± 13 Ma), in good agreement with previous work (e.g. Carlson, R.W., Lugmair, G.W. [2000]. Timescales of planetesimal formation and differentiation based on extinct and extant radioisotopes. In: Canup, R., Righter, K. (Eds.), Origin of the Earth and Moon. University of Arizona Press, Tucson, pp. 25–44). Younger zircon age domains (ca. 4530 Ma) also record crustal processes, but these are interpreted to be exogenous because they are well after the effective extinction of ^{26}Al ($t_{1/2}$ = 0.72 Myr). An origin via impact-resetting was evaluated with a suite of analytical impact models. Output shows that if a single impactor was responsible for the ca. 4530 Ma zircon ages, it had to have been ⩾10 km in diameter and at high enough velocity (>5 km s^{-1}) to account for the thermal field required to re-set U–Pb ages. Such an impact would have penetrated at least 10 km into Vesta's crust. Later events at ca. 4200 Ma are documented in HED apatite $^{235,238}U$–$^{207,206}Pb$ ages (Zhou, Q. et al. [2011]. Early basaltic volcanism and Late Heavy Bombardment on Vesta: U–Pb ages of small zircons and phosphates in eucrites. Lunar Planet. Sci. 42. Abstract #2575) and $^{40-39}Ar$ age spectra (Bogard, D.D. [2011]. Chem. Erde 71, 207–226). Yet younger ages, including those coincident with the Late Heavy Bombardment (LHB; ca. 3900 Ma), are absent from Millbillillie zircon. This is attributable to primordial changes to the velocity distributions of impactors in the asteroid belt, and differences in mineral closure temperatures (T_c zircon ≫ apatite).

1. Introduction

Impact records from the first billion years of Solar System history have been all but erased on Earth (e.g. Abbott et al., 2012; Abramov et al., 2013). Samples directly returned from the Moon by the Apollo and Luna missions, however, have provided the means to construct size–frequency/age relationships for various well preserved cratered surfaces. Due to this degree of preservation and as a consequence of direct sample returns as opposed to lunar meteorites that randomly sampled the lunar surface, the Moon serves as the baseline to which surface ages of solid objects have been derived for the inner Solar System (e.g. Stöffler and Ryder, 2001), and extrapolated to icy worlds of the outer Solar System (Zahnle et al., 2003; Chapman and McKinnon, 1986). The potential for asteroidal meteorites to provide a separate and independent

* Corresponding author at: Department of Geological Sciences, University of Colorado, UCB 399, 2200 Colorado Avenue, Boulder, CO 80309-0399, USA. Fax: +1 303 492 2606.
E-mail address: mojzsis@colorado.edu (S.J. Mojzsis).

http://dx.doi.org/10.1016/j.icarus.2014.08.025
0019-1035/

record of the impact environment of the inner Solar System from that of the Moon means that it makes sense to document ages recorded in different meteoritic minerals – and domains within these minerals – that are highly retentive and robustly preserve daughter-to-parent ratios of radiogenic systems. Such data could then be related back to models that describe and define the impact history of the wider Solar System (e.g. Morbidelli et al., 2012).

In this paper, we explored the thermal and temporal evolution of one of the largest asteroids, 4 Vesta, using zircon ($Zr(SiO_4)$) crystal chemistry and geochronology. This was accomplished via ultra-high spatial resolution (sub-micrometer) U–Th–Pb–Ti depth profile analyses in single crystals extracted from bulk samples of the brecciated eucrite Millbillillie. By measuring preserved $^{235-238}U/^{207-206}Pb$ ratios in different mineral domains (cores, mantles) within individual zircon grains (e.g. Mojzsis and Harrison, 2002), we show how the timing and extent of thermal events that affected them can be documented. If impact-produced recrystallized domains within meteoritic zircons can be correlated to previously reported radiometric ages for eucrites, other classes of asteroidal meteorites, martian meteorites, lunar rocks and ancient terrestrial rocks, it would help broaden our knowledge of the nature and extent of the earliest impact environments of the Solar System and fill in key gaps in our knowledge of the first hundred million years.

The asteroid belt as we know it emerged from the era of Solar System impacts; its overall structure appears to be a result of the early "hot" dynamical evolution of the inner Solar System that culminated in the so-called Late Heavy Bombardment, or LHB (e.g. Bottke et al., 2012; Minton and Malhotra, 2009, 2011; Morbidelli et al., 2012). The exact nature and timing of the LHB (also termed "impact cataclysm" *viz.* Tera et al., 1974) remains a topic of debate (Hartmann et al., 2000; Ryder, 2002; reviewed in Morbidelli et al., 2012; Norman and Nemchin, 2014). The origin and tempo of impacts prior to the postulated LHB, as well as before the Giant Impact that formed the Moon, and as far back as those associated with primary accretion of the planets, is even more mysterious.

2. Asteroidal meteorites as an archive of early Solar System bombardments

The world's catalogue of more than 50,000 meteorites is thought to be derived from approximately 110–150 distinct parent bodies in our Solar System (Burbine et al., 2002). The vast majority of these (>99.6%) are sourced from asteroids. An important meteorite group, the eucrites, are members of the so-called "E class" of the HED achondrites (howardites–eucrites–diogenites) which crystallized from melts in a large differentiated asteroid widely considered to be 4 Vesta (Keil, 2000). The battered surfaces of asteroids are testimony to a protracted history of collisions (Fig. 1), and Vesta is regarded as the only sizable object still left in the main belt with the spectral reflectance characteristics that could link it with the HEDs (McCord et al., 1970). It is worth noting that most HEDs are actually thought to originate not from Vesta itself, but from the group of Vesta family asteroids in the inner main belt between 2.1 and 2.5 AU dubbed "vestoids". These were originally linked to Vesta based on similarities in the compositions of HEDs and the surface mineralogy of Vesta as seen through spectroscopy (Binzel and Xu, 1993; Vilas et al., 2000; Burbine et al., 2001; McSween et al., 2011; McCoy et al., 2012). Most of the vestoid fragments may have been created ca. 1000 Myr ago during a colossal impact event that formed the large (500 km diameter) basin on Vesta named *Rheasilvia* (Marchi et al., 2012).

Dynamical observations connecting vestoids of the Vesta family to several escape hatches from the inner main belt, two of the most prominent being the 3:1 mean motion resonance with Jupiter at 2.5 AU and the υ6 secular resonance, provides a pathway for these asteroids to strike the Earth. This dynamical leakage makes them the most plausible source for the bulk of the HED meteorites that arrive to Earth. The HED meteorites have identical oxygen isotopic compositions, show similarities in mineralogy and composition (e.g. Fe/Mn elemental ratios of pyroxenes), and occur as polymict breccias (e.g. howardites contain fragments of diogenites and eucrites, etc.). As such, they derive from the same parent body (Papike et al., 2003; Wiechert et al., 2004; Greenwood et al., 2005; McSween et al., 2011).

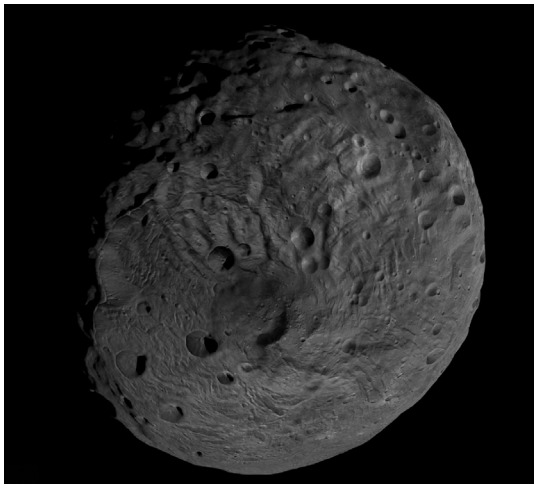

Fig. 1. The bombarded surface of 4 Vesta's south polar region as imaged by the framing camera on NASA's *DAWN* spacecraft in September 2011. Credit: NASA/JPL-Caltech/UCLA/MPS/DLR/IDA. The diameter of Vesta is approximately 530 km.

Generally speaking, the eucrites are igneous rocks (basalts and cumulates) or breccias composed of fragments of different igneous rocks termed "polymict breccias". Numerous whole-rock and mineral separates from eucrites have been dated using various long-lived and extinct radiometric systems ($^{40-39}Ar$, $^{207}Pb-^{206}Pb$, $^{182}Hf-^{182}W$, $^{53}Mn-^{53}Cr$, $^{147,146}Sm-^{143,142}Nd$, $^{87}Rb-^{86}Sr$, $^{26}Al-^{26}Mg$ and $^{60}Fe-^{60}Ni$) and the results of these studies show that the thermal history of Vesta and the V-types is complex (Nyquist et al., 1997; Tera et al., 1997; Ireland and Wlotzka, 1992; Bukovanská et al., 1997; Lugmair and Shukolyukov, 1998; Srinivasan et al., 1999; Carlson and Lugmair, 2000; Nyquist et al., 2001a,b; Bogard and Garrison, 2003; Misawa et al., 2005; Srinivasan et al., 2007; Bogard and Garrison, 2009; Zhou et al., 2013).

As is normally the case for rocks with such protracted histories of alteration, it has been difficult to discriminate between (i) ages that record igneous events associated with basaltic magmatism such as that produced from decay of short-lived nuclides, or (ii) partial to complete resetting of ages for different radiogenic isotope systems induced by metamorphism and/or impact heating. It is important to make this distinction so as to correctly interpret the geochronological output of the different radiometric systems noted above, and to draw inferences about impact events that affected the wider Solar System including early Earth.

Different accessory minerals show different responses to thermal events as a function of closure temperature; thus we may use these input parameters to inversely model impact conditions at different times in the past and eventually obtain a clearer picture of the early Solar System's impact environment. Eucrites have long been known (Rubin, 1997) to contain the accessory mineral phases zircon ($Zr(SiO_4)$), apatite ($Ca_5(PO_4)_3(OH,F,Cl)$), baddeleyite (ZrO_2), whitlockite ($Ca_9MgH(PO_4)_7$) and titanite (a.k.a. sphene; $CaTiSiO_5$) which also preserve daughter/parent ratios in the U–Pb system. The range of Pb diffusivity in these accessory minerals provides a means to reconstruct detailed thermal histories of the rocks

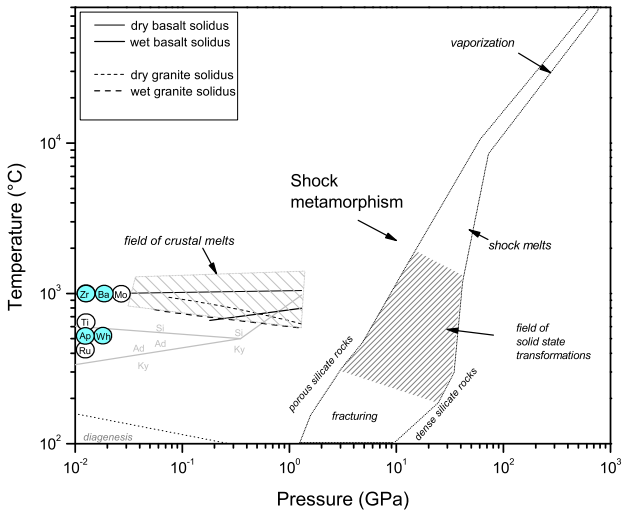

Fig. 2. Pressure–temperature fields for progressive impact metamorphism of silicate crusts in comparison to endogenic metamorphism of the terrestrial crust. Basalt and granite solidi are from Herzberg (1995). The terms Si–Ky–Ad correspond to the different Al_2O_3 polymorphs (sillimanite, kyanite, andalusite). Diagenesis represents the lowermost bounds of endogenic metamorphism. Upper curve of *P–T* field of shock metamorphism holds for porous regolith and regolith breccias (Heisinger and Head, 2006) and lower curves are for dense crustal rocks. The hatched field of solid state transformations is from Davies (1972). Shown are T_c values for important accessory mineral phases that have been identified in meteorites: zircon (Zr), baddeleyite (Ba), monazite (Mo), titanite (Ti), apatite (Ap) and rutile (Ru).

that host them. The concept of closure temperature (T_c) of a geochronological system can be described as is its temperature at the time corresponding to its apparent age. Hence T_c is a function of diffusivity, cooling rate and effective diffusion radius (Dodson, 1973). The condition of closure is that at a peak temperature equal to T_c, the mineral is not retentive of the diffusing species over short timescales, which can be constrained both by experimental and field-based empirical studies. Estimates for diffusion of Pb in zircon are for typical diffusion radii (1 μm–2 mm) and a cooling rate of 10 °C/Myr (Cherniak et al., 2004). Experimental work shows that T_c for igneous zircon is commonly above 1000 °C under these conditions. Fig. 2 shows a broad overview of the response of silicate crusts to various pressure–temperature fields for progressive impact heating compared to various terrestrial metamorphic facies. Although T_c has not yet been evaluated for another common meteoritic Zr-bearing accessory mineral – baddeleyite – field-studies indicate that it is near to that of zircon (Heaman and LeCheminant, 1993, 2000). Diffusion analyses in apatites provide consistent T_c of about 450–500 °C (Cherniak et al., 1991; Chamberlain and Bowring, 2000). Some closure temperature studies have also been performed for the common meteoritic phosphate phase – whitlockite – that indicate its response is similar to that of apatite (Mold et al., 1984; Sano et al., 2000). Studies of these complementary mineral systems are important areas of future research.

3. Sample description

It is evident from Fig. 1 that Vesta's igneous crust was subjected to impacts that excavated rocks from shallow, medium and deep depths into the asteroid. Impact-mixing of eucrites that originated in the crust and deeper mantle-derived diogenites, produced the various polymict breccias including the howardites and polymict eucrites cited above (Mittlefehldt et al., 1998). The eucrite meteorites investigated in this work were Camel Donga, Dhofar 1286, Dhofar 007, Millbillillie, NWA 1929, and NWA 2724 that come from the meteorite collection at the Department of Geological Sciences at the University of Colorado. The only sample in this collection that yielded analyzable zircons was from the Millbillillie meteorite.

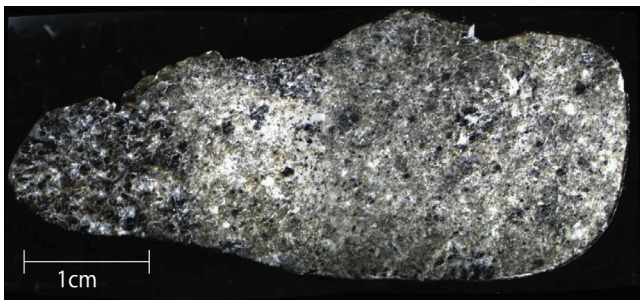

Fig. 3. Back-scattered electron (BSE) image of a thin section of the Millbillillie eucrite.

Millbillillie fell in 1960 near the town of Wiluna in Western Australia, and to-date has a total recovered mass of ~200 kg. It is classified as a monomict brecciated eucrite. Pioneering work from Bukovanská et al. (1997) reported zircons in Millbillillie that had a weighted mean $^{207}Pb/^{206}Pb$ age of 4560 Ma when pooled with zircon ages derived from 4 other eucrites: Juvinas, Cachari, Jonzac, and Pasamonte. Reported ^{244}Pu–Xe ages suggest that Millbillillie is composed of a mixture of materials which yield different ages of 4507 ± 21 Ma and 4566 ± 24 Ma for coarse-grained and fine-grained sections, respectively (Miura et al., 1998). The two pieces of Millbillillie in our collections (7.0 and 8.3 g) contain coarse-grained and fine-grained clasts of mainly pyroxene and plagioclase with lesser amounts of ilmenite; regions of granulitic breccia and impact melt from later recrystallization episodes are also apparent in hand samples (Fig. 3). Of the four zircons (7–40 μm) extracted from these samples, all are in contact with larger ilmenite and pyroxene crystals (Fig. 4). As previously mentioned, this association with ilmenite (general form: $Fe(TiO_3)$) undermined the reliable use of Ti-in-zircon thermometry (Watson and Harrison, 2005). Backscattered-electron (BSE) images of one zircon (mb1_gr) reveal that it is compositionally inhomogeneous (Fig. 5) whereas the other zircons examined showed mundane internal structure.

4. Analytical techniques

4.1. Sample preparation and documentation

Our intent was to probe the conditions under which different domains within individual zircon crystals could have formed after the primary crust solidified on Vesta very early in its history. To do this required that the largest possible individual zircon grains be extracted. Bulk meteorite samples were divided into three parts: one was used for preparation of standard petrographic thick (100 μm) sections, a separate split was crushed for heavy mineral extraction (see below), and the main mass was retained and archived. Thick sections were examined for zircons by transmitted and reflected optical microscopy and thereafter scanned on a LEO 1430 VP scanning electron microscope with an energy-dispersive analyzer at the UCLA National Ion Microprobe Facility. No zircons were found in the thick section mounts we examined. The second fraction was gently crushed by hand in pre-cleaned agate mortars to fine powders, sieved in dedicated nylon sieves, and passed over with a hand magnet to concentrate non-magnetic fractions prior to density separations. Heavy minerals – including zircon – were isolated using heavy liquid techniques (reagent-grade Geoliquids©

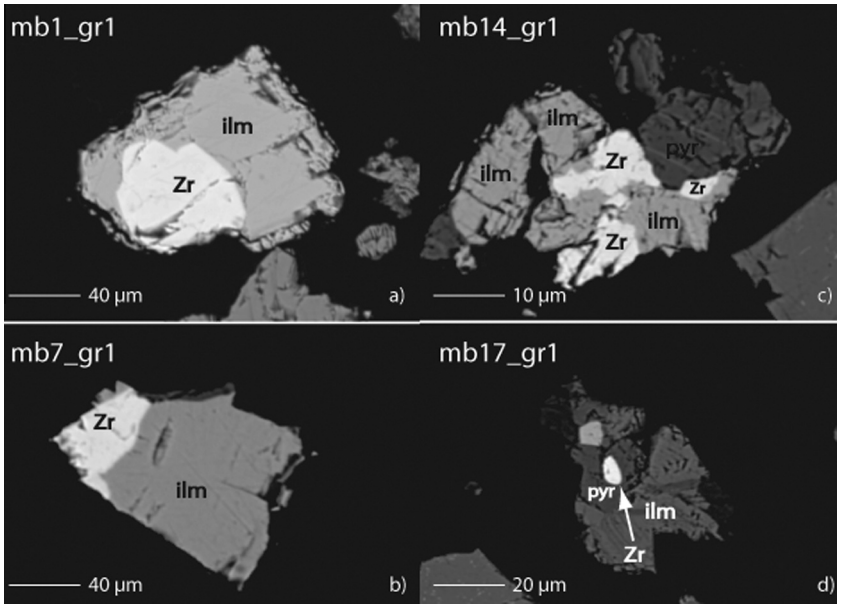

Fig. 4. BSE images of Millbillillie zircons in contact with ilmenite and/or pyroxene grains.

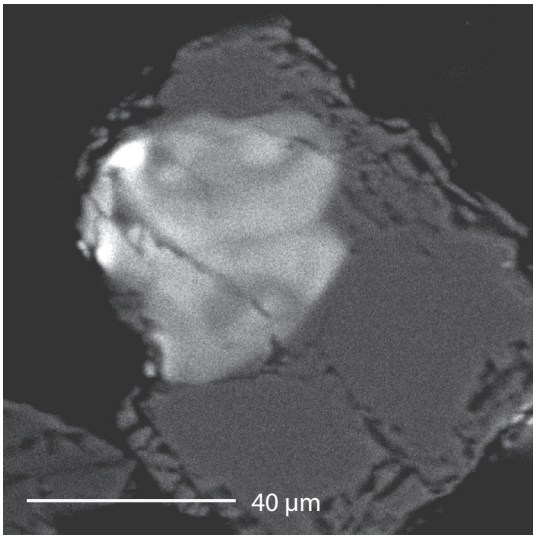

Fig. 5. BSE image of zircon mb1_gr1 that shows inhomogeneous composition from differences in electron image contrast.

methylene iodide). After extraction, the heavy mineral fraction was cleaned in successive acetone and deionized water baths and carefully sprinkled into a cleaned glass funnel directed onto double-sided adhesive tape. The remainder was stored for future use. This procedure created a 0.8 cm^2 circular mono-layer ("sprinkle mount") of high-density minerals. Hand-picked zircon standards (AS-3; Paces and Miller, 1993; Black et al., 2003; Schmitz et al., 2003) were placed in a halo around the grain target, and the entire assembly was cast together in 2.2 cm diameter Buehler© epoxy disks. Because of the low sample volume and small grain size of most of the zircons thus far discovered (generally ~10 µm) we found that the method of casting all the heavy-mineral separate together – winnowed to within the density range of zircon – yields better results than the guesswork involved with individual grain picking of very rare zircon. After hardening in a 50 °C vacuum oven, the epoxy disks were removed from their adhesive backing, cleaned in distilled water and lightly hand polished using 6–0.25 µm alumina paste in stages until grains were exposed. The grain mounts were then mapped optically (transmitted and reflected light) and by BSE, and the image maps were used to plan ion microprobe analysis.

4.2. U–Th–Pb–Ti ion microprobe depth profiles

All depth-profile U–Th–Pb geochronology was performed on the UCLA Cameca ims1270 ion microprobe in monocollection mode following standard procedures (e.g. Cates and Mojzsis, 2009; Abbott et al., 2012). Optical and electron images of the grains were created prior to depth profile analysis to help determine the target area in which to begin sputtering on the grain as well as to avoid cracks, inclusions, and other imperfections which have the potential to show erroneously high degrees of Pb^* loss or contamination. After imaging studies were completed, the mount was gently re-polished by hand for <30 s using a 0.25 µm alumina colloidal suspension, cleaned in alcohol and distilled water baths and allowed to air dry in an oven at 55 °C. The sample was then Au sputter-coated to ensure a conductive surface.

None of the Millbillillie zircons in our samples displayed euhedral, or even subhedral habit. Furthermore, because our Millbillillie zircons were small, they could not be plucked from the polished epoxy grain mounts as is conventionally done for depth profiling (Mojzsis and Harrison, 2002; Trail et al., 2007) because they were deemed too thin and fragile to remove from the target mounts for re-mounting without risk of disintegration. Instead, the zircons remained in their epoxy target mounts along with co-existing polished AS3 standards and depth-profiled from the "inside-out". More about this method follows.

Both $^{235,238}U$ and ^{232}Th concentrations were obtained first in the conventional ion microprobe "spot mode" via comparison to a working curve constructed using $^{238}U^+/^{94}Zr_2^{16}O^+$ and $^{232}Th^+/^{94}Zr_2^{16}O^+$ in the eucrite zircon unknowns with those in zircon standard 91500 (U = 81.2 ppm; Th/U = 0.3; Wiedenbeck et al., 2004). This was done because our usual AS-3 zircon geochronology standard shows highly variable U and Th abundances (Black et al., 2003) rendering it unsuitable as a U and Th concentration standard.

Long-duration profile analyses of very small meteoritic zircons presented a considerable analytical challenge. Normally, the depth

profile method makes use of previously analyzed zircons that have been removed from their original mounts and re-cast with the unpolished side up. Depth profiles are then initiated from the "outside-in", or from "rim to core" so that they sample in the reverse order of sense of growth in the zircon. Owing to the fragility of our samples, all depth-profiles reported in this work were instead initiated in the core regions of already polished meteoritic zircons and profiled towards the outside rim of the zircon grain so as to create "inside-out" depth profiles. This technique not only works well for depth-profiles in general, but also avoids several common technical problems inherent in the standard approach as originally described in Mojzsis and Harrison (2002). Because the reflected light optics and imaging capability of the Cameca ims1270 SIMS is poorly suited for high-resolution microscopy, a recurring challenge to the depth profile technique has been to accurately relocate spots for targeted analysis once the sample is in the instrument. These problems are rendered moot with the new "inside-out" approach taken here because the profile always begins on a uniform polished surface at maximum crystal exposure, and it is thus trivial to re-locate the spot for continued analysis. Contamination from common Pb and Ti from the sample preparation process is also minimized in this way because the mount has already been cleaned, polished and pre-sputtered.

The internal distributions of U–Th–Pb in each zircon were obtained utilizing a 15 kV, ~5 nA $^{16}O^-$ primary beam defocused to a ~25 μm spot for extended periods. The analytical sessions in depth profiling mode consist of a continuous collection of 50–200 ion microprobe cycles which corresponds to pit depths of several micrometers. Since it is established that internal error increases with increasing pit depth due to changes in ion counts and other factors (Trail et al., 2007), depth profile runs were concluded before 200 cycles were completed (see below). In the data analysis, cycles from each of the four depth profile analyses were grouped to define a single data block (1 block = 10 cycles). A depth profile from a ~100% concordant zircon standard (AS-3) cast in each mount was used to correct for induced errors from increasing pit depth as a function of depth of the pit into the crystal via a MicroXAM© surface profilometer (10 cycles were found to correspond to 0.38 μm; Supplementary Table S2. Zircon grains mb1_gr1 and mb7_gr1 were analyzed in session 1, and mb14_gr1 and mb17_gr1 in session 2 (Supplementary Table S1). All U–Pb plots were generated using the Isoplot software package (Ludwig, 2003), with results reported in Supplementary online materials (Fig. S1; Tables S1 and S2).

Although it was found that the Pb–Pb age and Th/U ratio remain constant with depth for a concordant and isotopically homogeneous grain during a zircon depth profile, Trail et al. (2007) noted a predictable inter-element discrimination that occurs due to varying ion counts of Pb and U as a function of depth. This secular change influences the apparent U/Pb concordance calculation (i.e. [^{206}Pb/^{238}Pb age]/[^{207}Pb/^{235}Pb age] * 100, expressed as % concordance). To monitor and correct for this effect, we performed a depth profile for mb1_gr1 for 200 cycles (7.69 μm) and exactly the same experimental condition was applied to a neighboring zircon standard grain AS-3 for 100 cycles (3.8 μm). The degree of apparent concordance vs. depth for mb1_gr1 follows a function that changes slope sign after about 3 μm into the crystal, whereupon apparent concordance decreases from ~100% to 70% (Fig. 6). Afterwards, apparent concordance increases from 3 to 7.5 μm depth and ends at a value of ~100%. The 100-cycle profile of standard AS-3 shows a near-identical trend, with a slight offset (Fig. 6). This offset is to be expected in the data, as mb1_gr1 is less concordant than AS-3. Because apparent concordant variations are the result of a change in the ion yields of U, UO, and Pb with depth of the sputter pit, in a homogeneous grain the relative ion yields of Pb isotopes should vary little with pit depth. This is similar to how

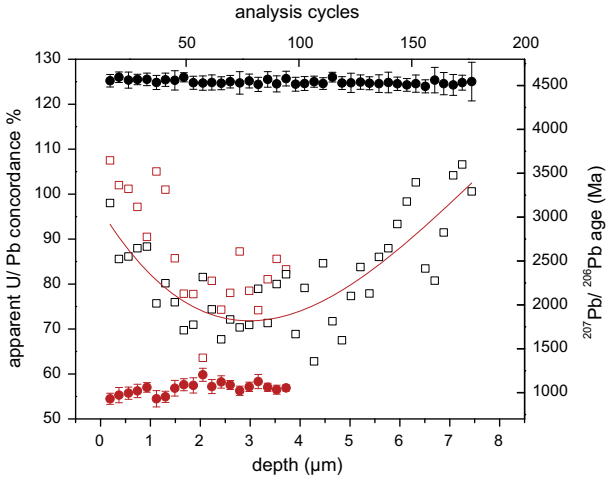

Fig. 6. Profile of zircon sample mb1_gr1 fitted with 3rd order polynomial allowing for a correction for the instrumental fractionation effect from increasing pit depth. This was used to estimate zircon concordance with depth for all zircon depth profiles reported herein. This effect can be monitored by a comparison of a depth profile for mb1_gr1 (200 cycles, black open squares) to concordant zircon standard AS-3 (100 cycles, red open squared) under identical experimental conditions. Note the ^{207}Pb/^{206}Pb ages for both mb1_gr1 (black circles) and AS-3 (red circles) remain invariant with depth of pit. (For interpretation of the references to color in this figure legend, the reader is referred to the web version of this article.)

a Pb^+, U^+ vs. UO^+/U^+ calibration line has no bearing on the Pb–Pb age. Fig. 6 proves this point and demonstrates that there is little to no variation in the Pb/Pb age with respect to depth for both the mb1_gr1 and AS-3 depth profiles. The apparent concordance vs. depth profile of sample mb1_gr1 can be fitted with a third order polynomial and this correspondence can be used to correct apparent discordance for pit depth and reveal the true concordance of the unknown grain. The shape of the polynomial curve will likely vary from analytical session to analytical session (similar to the variation of the Pb^+, U^+ vs. UO^+/U^+ calibration line), so that a comparison of AS-3 depth profiles vs. mb14_gr1 and mb17_gr1 depth profiles was repeated for session 2; in that case the experiment yielded similar results.

5. Results

5.1. U–Pb depth profile geochronology

5.1.1. Mb1_gr1 zircon

Zircon mb1_gr1 was continuously analyzed for 200 cycles corresponding to a ~8 μm depth profile (Fig. 7a). The depth profile appears to show two Pb–Pb age plateaus which may represent two distinct events (see Section 5). The first preserves a concordant ^{207}Pb–^{206}Pb core age of 4555 ± 17 Ma (2σ; MSWD = 0.71; n = 10 analysis blocks) up until 4 μm depth, then drops to a ~4 μm-wide rim domain age at 4531 ± 20 Ma (2σ; MSWD = 0.59; n = 10).

5.1.2. Mb7_gr1 zircon

Grain mb7_gr1 (Fig. 7b) was depth profiled for ~5 μm and shows one domain ^{207}Pb–^{206}Pb age of 4537 ± 18 Ma (2σ; MSWD = 0.65; n = 14) over the 135 analysis cycles.

5.1.3. Mb14_gr1 zircon

A ~3 μm (75 cycles) depth profile of grain mb14_gr1 shows one domain ^{207}Pb–^{206}Pb age of 4520 ± 70 Ma (2σ; MSWD = 0.26; n = 8) (Fig. 7c).

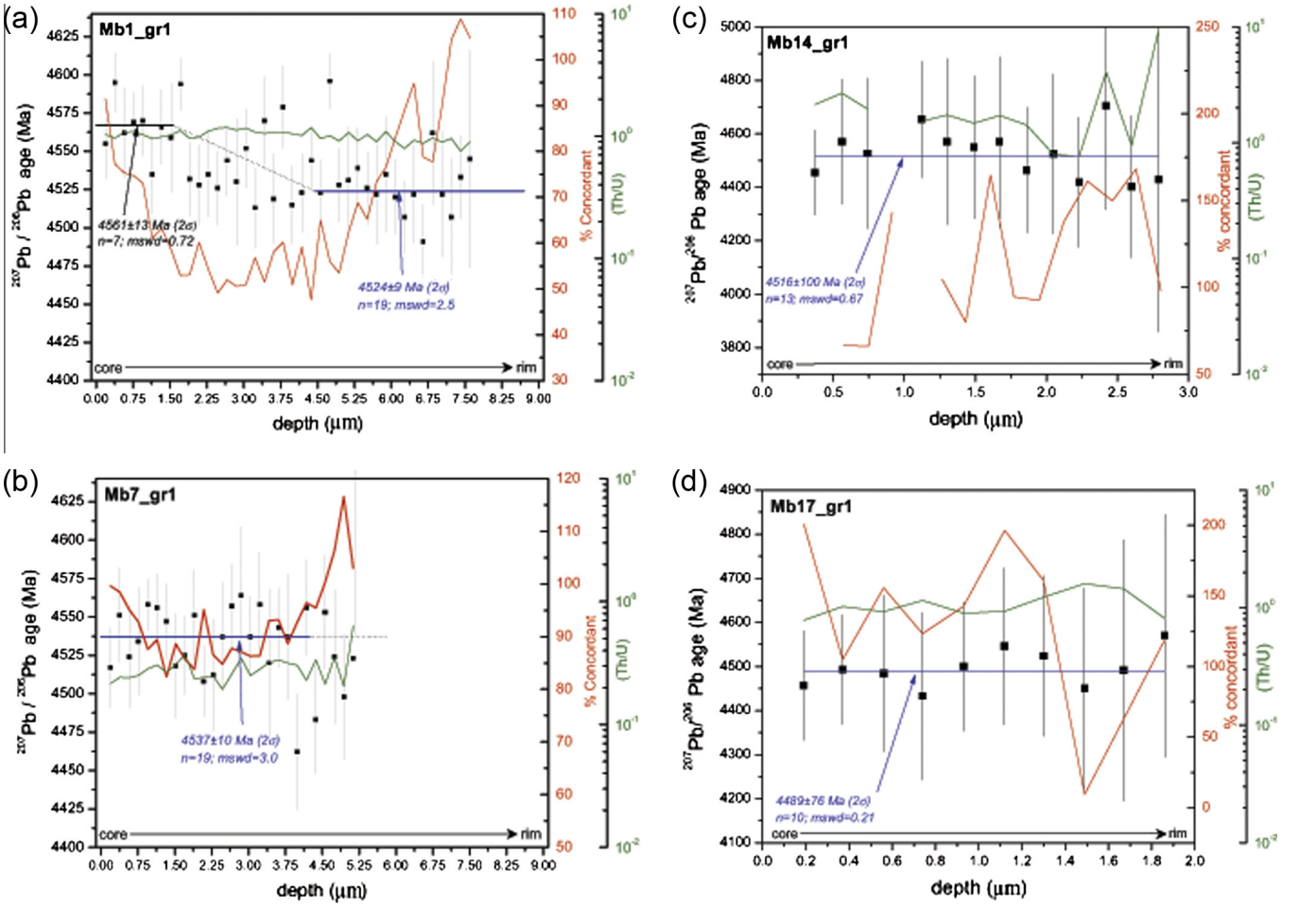

Fig. 7. Results from $^{207}Pb/^{206}Pb$ vs. depth plots of all analyzed grains (black squares indicated age variation with depth at the 1σ level, blue line shows age analyses included in weighted mean); Pb^{*} concordance vs. depth is represented by the solid red line, while apparent concordance (before the correction was applied) is represented by the dashed red line. Th/U values and their errors are shown in green. (For interpretation of the references to color in this figure legend, the reader is referred to the web version of this article.)

5.1.4. Mb17_gr1 zircon

Grain mb17_gr1 was depth profiled for ~2 μm (50 cycles) with one domain ^{207}Pb–^{206}Pb age of 4494 ± 52 Ma (2σ; mswd = 0.28; n = 5; Fig. 7d).

5.2. U–Pb concordance and Th/U related to zircon depth profiled regions

Changes in Th/U ratios ($[Th/U]_{zrc}$) and U–Pb isotopic concordance with depth can be used to probe the timing of new growth or alteration/modification of pre-existing zircon (Cates and Mojzsis, 2007; Mojzsis and Harrison, 2002). These changes arise from the chemical partition between the zircon and melt during diffusional magmatic exchange, solid-state recrystallization, or zircon and fluid exchange during metamorphism. While the degree of U–Pb concordance allows us to determine if mineral domains within the zircon have remained closed (i.e. no exchange of U and Pb with the environment), the $[Th/U]_{zrc}$ is a separate crystal-chemical monitor of external processes that affect the zircon.

For session 1, the results of $[Th/U]_{zrc}$ vs. Pb–Pb dates for grain mb1_gr1 show that $[Th/U]_{zrc}$ gives a value ranging from ~0.8 to 1.1 (Fig. 7a). The U/Pb corrected concordance % of mb1_gr1 and mb7_gr1 remains concordant throughout the profile (Fig. 7a and b). The $[Th/U]_{zrc}$ for mb7_gr1 shows a variation from 0.2 to 0.5 throughout the depth profile (Fig. 7b).

In session 2, mb14_gr1 displays a scatter of $[Th/U]_{zrc}$ values from 0.4 to 9.4 (Fig. 7c), while results for mb17_gr1 show smaller variations in $[Th/U]_{zrc}$ with values that range from 0.9 to 1.6 (Fig. 7d). The U/Pb concordance % for both mb14_gr1 and mb17_gr1 is highly variable. They have not had an IMF correction applied to their profiles because the AS3 profiles and the unknown profiles do not exhibit the same behavior through the depth profile (Fig. S2). Thus the geological significance with respect to concordance cannot be evaluated in this particular example.

6. Discussion

6.1. Interpretation of Millbillillie zircon depth profile geochronology

The ion microprobe depth-profile session 1 for grain mb1_gr1 shows a core age (4555 ± 17 Ma; 2σ), which overlaps in time with other more precise Pb–Pb ages previously reported for Millbillillie (Bukovanská et al., 1997). We postulate that a second age domain is present in grain mb1_gr1 that corresponds to 4531 ± 20 Ma (2σ), an age that is similar to the young age obtained for grain mb7_gr1 (4537 ± 18 Ma; Section 5.1.3). Since the two age plateaus in the mb1_gr1 profile are close in age to one another when the margin of error is considered, we applied a statistical K–S (Kolmogorov–Smirnov) test to determine whether these two ages differ in a statistically significant way. The aim of the K–S test is to assign num-

bers to the test results; *P*-values report if the numbers differ significantly and we can reject the null hypothesis if *P* is "small" (<0.05). In applying the K–S test, the 20 analysis blocks collected during the mb1_gr1 depth profile were split in half to define each of the dataset values of 10 blocks each. Results show that the maximum difference between the cumulative distributions (*D*) is 0.7000 with a corresponding *P* of 0.007; thus suggesting that the two ages are statistically different. Student's *t*-test was also applied to these data and yielded similar results with a *P* value of 0.002.

Two different age populations in the mb1_gr1 data are statistically plausible, the next step is to determine how the younger zircon mantle could have formed onto the older existing core. The fact that the age domain from mb7_gr1 (4537 ± 18 Ma) is similar to the younger mantle age seen in mb1_gr1, means that an explanation must exist as to why both zircon ages are present in the same grain of the same rock from an asteroid that was effectively geologically moribund after the extinction of ^{26}Al at about 5 Myr after Solar System formation.

Admittedly, the significant analytical challenges associated with depth profiling such small grains as mb14_gr1 and mb17_gr1 in our analytical session 2 mean that these data are of lower quality. Results from mb14_gr1 yielded a ^{207}Pb/^{206}Pb age of 4516 ± 100 Ma (2σ) and mb17_gr1 has a ^{207}Pb/^{206}Pb age of 4489 ± 76 (2σ). Both zircon ages are so imprecise that they overlap with both the primary crystallization and rim age domains reported in mb1_gr1 and mb7_gr1 and are therefore not useful in our model for the formation of different zircon ages in Millbillilie.

We now consider four plausible formation scenarios to explain how a younger zircon age domain could be present in mb1_gr1 that is the same as the domain age in mb7_gr1 (about 30 Myr after crystallization of Vesta's crust):

(i) younger magmatic overgrowths formed from recrystallization in an impact-generated melt;
(ii) younger magmatic overgrowths arose from recrystallization from continued (late) basaltic magmatism in Vesta;
(iii) diffusion-controlled age resetting from impact shock heating resulted in these different zircon age domains; or
(iv) metamorphic overgrowth not related to shock effects from impact (non-shock metamorphism associated with fluids in the asteroid's crust) generated these younger age domains.

We made use of both compositional ($[Th/U]_{zrc}$) and geochronological (U–Pb concordance) data from our four zircons to distinguish between the different scenarios cited above. Values of $[Th/U]_{zrc}$ for mb1_gr1 range from ~0.8 to 1.1 (Fig. 7a), while the corresponding values for mb7_gr1 vary from 0.2 to 0.5, and mb17_gr1 from 0.9 to 1.1. In Earth rocks, the range of $[Th/U]_{zrc}$ values from ~0.5 to 1.0 are consistent with exchange equilibrium of U and Th with zircon grown in an igneous (melt) environment (Hoskin and Schaltegger, 2003). Although the $[Th/U]_{zrc}$ from mb14_gr1 has a slightly wider range (0.4–9), the large internal errors muddle interpretation. Our first order assessment of $[Th/U]_{zrc}$ suggests that scenario (iv; non-shock metamorphism induced by fluids) was not responsible for the 4530 Ma age seen in mb1_gr1 and mb7_gr1 zircons because a much higher degree of variability in $[Th/U]_{zrc}$ is expected under such fluid-mediated circumstances (e.g. Mojzsis and Harrison, 2002). Fortunately, whole rock compositional data are available for various fragments of Millbillillie (Shukolyukov and Begemann, 1996; Miura et al., 1998) that can be compared with the chemistry of the eucrite zircons. We find that the range of $[Th/U]_{zrc}$ for the mb1_gr1 zircon (0.8–1) is consistent with exchange equilibrium of bulk Millbillillie melt with $[Th/U]_{WR}$ = 4.45 as reported in Shukolyukov and Begemann (1996). If we assume $D_{Th/U}^{zircon/melt} = 0.2$ (e.g. Mojzsis and Harrison, 2002 and references therein), the predicted $[Th/U]_{zrc}$ = 0.89 agrees well with the mean of measured values (0.9) shown in Fig. 7a. This result appears to weaken scenario (iii) which requires the zircon to have formed from diffusion-controlled age resetting because the expectation is that Th and U would also be mobilized under such conditions. It renders scenario (iv) as implausible for the younger age shared by mb1_gr1 and mb7_gr1 because non-magmatic $[Th/U]_{zirc}$ (i.e. values that cannot be reconciled with the whole-rock compositions) are not observed. Owing to the fact that scenarios (i) and (ii) would yield similar $[Th/U]_{zrc}$ values, however, we can cannot distinguish between the two using this criterion. Conversely, the single age domain in mb7_gr1 (Fig. 7b) preserves consistently lower $[Th/U]_{zrc}$ values (0.2–0.5), which cannot be explained via simple partial melting and/or with exchange equilibrium of bulk Millbillillie melt ($[Th/U]_{WR}$). The composition of mb7_gr1 does, however, comport with the [Th/U] composition of Millbillillie matrix (0.2–0.7; Miura et al., 1998). We interpret this to mean that scenarios (i), (ii) and (iv) are the least-likely explanations for the origin of the young age of mb1_gr7 that resembles the young age in mb1_gr1. This analysis leaves scenario (iii), diffusion-controlled age resetting of zircon from impact, as a distinct possibility.

Finally, the corrected U/Pb concordance % for grains mb1_gr1 and mb7_gr1 remain broadly concordant throughout the depth profiles (Fig. 7a and b). Although this feature rules out scenario (iv), it provides a non-unique solution to distinguish between scenarios (i)–(iii). Apparent U/Pb concordance % was highly variable throughout each depth profile in grains mb14_gr1 and mb17_gr1.

6.2. Analytical impact models of thermally-induced zircon age resetting on Vesta

In this section, we present the output of an analytical method (e.g. Abramov et al., 2013) to assess impact heating as a means to evaluate the probability of impact-induced age resetting in zircon from scenario (iii) in Section 6.1. The goal was to probe the likelihood that impact-generated melt sheets could be produced on Vesta after its formation such that these thermally alter the asteroid's crust to the degree that zircon ages could be re-set. The model also assesses the likelihood that a single large event – rather than multiple smaller events – could have been responsible for radiometric ages younger that the crystallization ages of Vesta's crust.

A key parameter in calculating post-impact temperature distributions is shock pressure as a function of distance from the center of impact, which follows the power law:

$$P = A\left(\frac{r}{R_p}\right)^{-k} \quad (1)$$

where R_p is the radius of the projectile, r is distance, k is the decay exponent, and A is pressure in the isobaric core, which approximately corresponds to the radius of the projectile (e.g., Pierazzo et al., 1997; Pierazzo and Melosh, 2000). The decay exponent k varies with impact velocity such that:

$$k \approx 0.625 \log(v_i) + 1.25 \quad (2)$$

with v_i in kilometers per second (Ahrens and O'Keefe, 1977). Initial shock pressure A is based here on an estimate by Collins et al. (2002) and corrected for the impact angle θ using the results of Pierazzo and Melosh (2000):

$$A = \frac{\rho v_i^2}{4} \sin\theta \quad (3)$$

where ρ is impactor and target density, both of which are assumed to be about 3000 kg m^{-3}. This value was chosen because it is consistent with estimates of Vesta's bulk silicate density from results of

the *DAWN* mission (Russell et al., 2012) and the measured bulk densities of HED meteorites (Britt et al., 2010). This density is also generally appropriate for rocky impactors. An impact angle of 45° is assumed due to it being the most probable impact trajectory (Gilbert, 1893; Shoemaker, 1962).

In the model, shock pressure is converted to a temperature increase using an expression for specific waste heat (ΔE_w) based on the Murnaghan equation of state (Kieffer and Simonds, 1980). Vesta's crust has an approximately basaltic composition (e.g. McCord et al., 1970), so that the requisite parameters for basalt as given by Kieffer and Simonds (1980, and references therein) were used in our model. To obtain the temperature increase ΔT, the specific waste heat ΔE_w is divided by the heat capacity of the target rock, which is ~800 J kg^{-1} K^{-1} for basalt. To obtain the final post-impact temperature distribution, ΔT is added to the internal temperature of Vesta, which is estimated at −95 °C based on *Herschel* mission observations of the surface temperature (Leyrat et al., 2012) and modeled diurnal averages (e.g., Müller and Lagerros, 2003).

Parameter space for impactor diameters (km) and velocities (km s^{-1}) were modeled in increments of 1 km and 1 km s^{-1}, respectively, between values of 1 and 50. For each parameter combination, temperatures were calculated as a function of distance from the impact point, and volumes of material that exceeded the threshold temperature needed to age-reset zircon were determined. The closure temperature (T_c) is based on Pb diffusion behavior in zircon (Cherniak and Watson, 2001) and varies depending on the size of the mineral grain and the exposure time at a given temperature. For the >50 μm^3 grains analyzed in this work, predicted reset temperatures range from ~1000 °C for zircons emplaced several kilometers underneath the surface, to ~1200 °C for zircons in a 100 m thick surface ejecta blanket (Abramov et al., 2013); an intermediate value of ~1100 °C was used in the calculations here.

The results, shown in Fig. 8, show that the impact velocity needed to achieve any age-resetting in zircons on Vesta must far exceed 5 km s^{-1}. The mean velocity of asteroids striking Vesta in the pre-LHB time period is estimated as somewhat less than this (4.67 km s^{-1}; Marchi et al., 2013), which means that faster-than-normal impacts were necessary to meet or exceed T_c. Our results show that most age resetting of the U–Pb system in zircon should have been caused by impactors striking at velocities greater than ~10 km s^{-1}. The probability of a projectile hitting Vesta at impact speeds >10 km s^{-1} is relatively low, but the volume of reset material made by such impacts increases sufficiently that one would expect many impact-generated zircon U–Pb age-resetting events to have been made by such projectiles (Marchi et al., 2012, 2013).

Although the results presented in Fig. 8 suggest that a 50 km diameter, 50 km s^{-1} impactor can age-reset a large percentage of Vesta's volume (~20%), the very low probability of such an impact coupled with the question of whether Vesta would have mechanically survived such an event (Fig. 9) render this scenario unlikely. The three panels shown in Fig. 9 re-create the relevant parts of Marchi et al. (2012, their Fig. S3). The top panel in Fig. 9 shows how the baseline output from the analytical code results in significantly higher temperatures than the hydrocode. The middle panel accounts for the vertical component of impact velocity only as per Marchi et al. (2012); we note that the energy deposited by the hor-

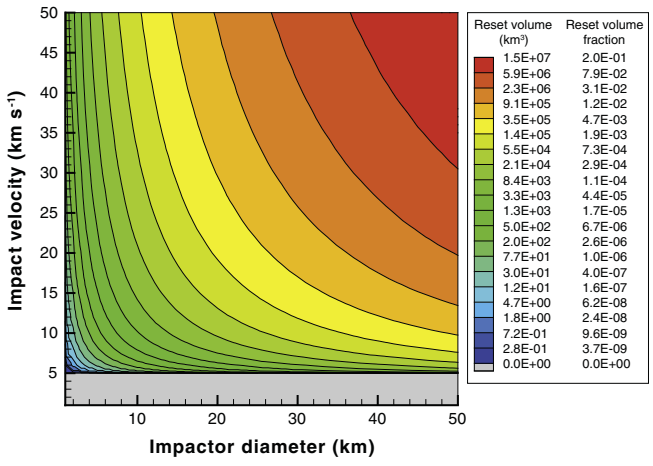

Fig. 8. Volume shock-heated to a temperature required for complete age-resetting in zircon (~1100 °C) as a function of impactor diameter and velocity. Reset volume is expressed as both km^3 and as a fraction of Vesta's total volume.

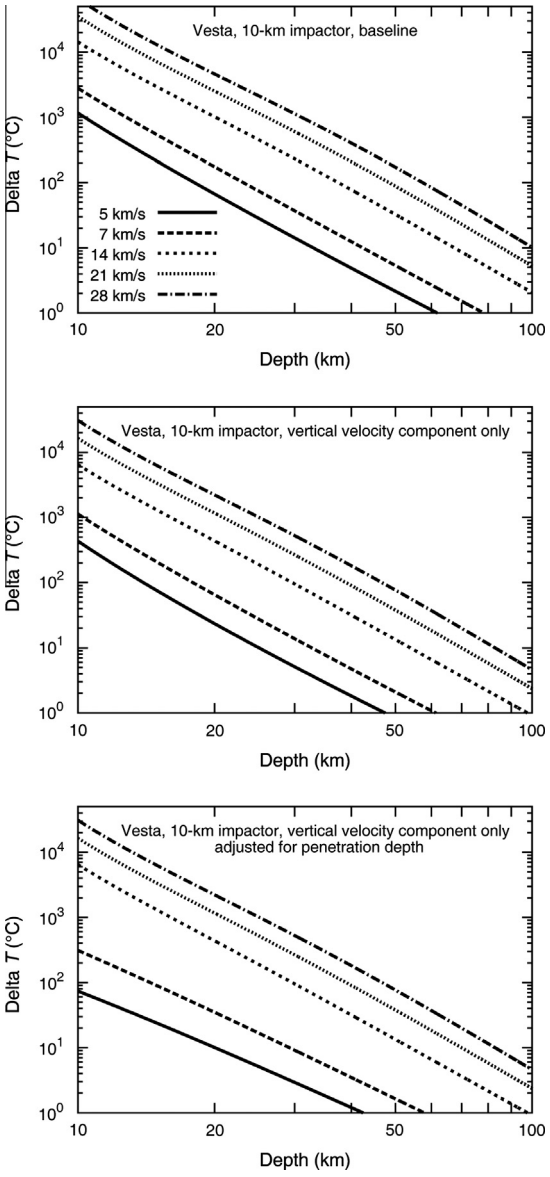

Fig. 9. Results of our analytical models of the bombardment of the Vesta under different impact regimes. The top panel shows the output from our baseline model that resulted in significantly higher temperatures than the hydrocode model reported in Marchi et al. (2012). However, after considering only the vertical component of impact velocity the match between the two models was significantly improved (middle panel). The final correction (bottom panel) was for the location of the impact center, which shows that faster impacts penetrate deeper into the subsurface. This has little effect on age-reset volumes, but does affect temperature as a function of depth.

izontal velocity component should not be neglected. The final correction to our model (Fig. 9, bottom panel) was for the location of impact center. Faster impacts penetrate deeper into the subsurface which appears to not affect age-reset volumes very much, but does affect temperature as a function of depth. After the necessary corrections outlined above, the analytical method matches the hydrocode results quite well and lends confidence to the output generated in Fig. 8.

The impact structure *Rheasilvia*, at 505 km in diameter, is the largest so far documented on Vesta. Its size corresponds to a projectile diameter of ~37 km for a 10 km s^{-1} impact, or ~15 km for a 50 km s^{-1} impact, assuming an impact by a rocky asteroid and using π-group scaling laws (Schmidt and Housen, 1987) and the Croft (1985) final-to-transient crater relationship. The model predicts that at 10 km s^{-1}, the *Rheasilvia* impact event would have been sufficient to age-reset (in zircon) only ~0.2% of Vesta's volume and ~1% of its surface area. If age-resetting in the $^{40-39}$Ar system is considered, these values are 40–60% higher due to a lower reference temperature of 727 °C (Marchi et al., 2012). In addition, Vesta's low escape velocity of ~0.35 km s^{-1} would likely cause a substantial fraction of high-energy, hot, age-reset ejecta to be permanently lost. If *Rheasilvia* is as young as has been argued (~1000 Ma), and most HED meteorites actually originate from the Vestoids that formed earlier than *Rheasilvia*, this would explain why such a young age is absent from our analyses.

6.3. Thermal and bombardment history of Vesta as seen through other radiometric systems

Vesta's initial formation, where timing is constrained by short-lived chronometers such as Hf–W, Mn–Cr and Al–Mg, took place within the first few million years of Solar System history (Srinivasan et al., 1999; Carlson and Lugmair, 2000; Nyquist et al., 2001a,b). The ^{53}Mn–^{53}Cr abundances from the basaltic eucrite Chervony Kut yields an age of 4563.6 ± 0.9 Ma, which is only about 4 Myr younger than the formation of CAIs (Lugmair and Shukolyukov, 1998). Further studies using ^{26}Mg from the decay of ^{26}Al (half-life 0.73 Myr; Srinivasan et al., 1999; Nyquist et al., 2001a,b) and ^{60}Ni from the decay of ^{60}Fe (half-life 1.5 Myr; e.g. Tang and Dauphas, 2012), whole rock $^{40-39}$Ar ages of unbrecciated eucrites (Bogard and Garrison, 2003), and Hf–W data (Kleine et al., 2004) also support the interpretation that early crust formation occurred probably about 3 Myr after CAI formation; this is consist both with accretion timescales for the planetesimals, and of Mars (Kita et al., 2005; Kleine et al., 2009; Dauphas and Pourmand, 2011). In addition, thermal models based on the decay of short-lived nuclides predict formation times relative to CAI formation that are broadly consistent within constraints for accretion (2.85 Myr), core formation (4.58 Myr) and solidification of crust (6.58 Myr) on Vesta (Ghosh and McSween, 1998).

Other isotopic systems applied to whole-rock and mineral samples such as U–Pb, Pb–Pb, ^{147}Sm–^{143}Nd, ^{40}Ar–^{39}Ar have previously been examined to constrain formation times, subsequent basaltic magmatism, and later impact heating and metamorphism for the HED meteorites (Wadhwa and Lugmair, 1996; Bogard and Garrison, 2003; Misawa et al., 2005; Nyquist et al., 2008; Zhou et al., 2013); these studies yield a wide range of ages (Fig. 10). For instance, Zhou et al. (2013) reported U–Pb and Pb–Pb ages of non-cumulate basaltic eucrite zircons in Béréba, Cachari, Caldera, Camel Donga, and Juvinas that they viewed were consistent between mean Pb–Pb age and mean U–Pb concordia age; their interpretation was that there was insignificant Pb-loss from thermal heating in HED zircons. These authors proposed, however, that a small spread in ages likely represents Vesta's initial core–mantle differentiation at ~4564 Ma followed by peak basaltic magmatism at ~4552 Ma that gradually diminished over the next 50 Myr. We wish to point out that this is not the only plausible formation scenario that would yield such results. If zircons formed under the conditions in our scenario (ii) described in Section 5.1, where younger zircon grew in an impact-generated melt, we would expect the U–Pb and Pb–Pb ages to be similar. In addition, the variability in the Th/U ratios (0.05–3.57) from the largest zircon population (Camel Donga) reported in Zhou et al. (2013) supports (iii) and (iv) as possible formation scenarios.

As previously mentioned, no Eucrite zircons thus far found appear to record events coinciding with either a ca. 4200–4300 Ma events recorded on the Moon and eucrite apatites, nor with the later Solar System-wide LHB at about 4100–3900 Ma. This lack of later records of impacts may be due to Vesta's small size (~530 km diameter), locally low impact velocities (<5 km s^{-1}) at its contemporary semi-major axis distance from the Sun (2.36 AU), and fewer high velocity impacts than during early bombardment.

6.3.1. Bombardment of the asteroids vs. the Moon

The growing database of ages for various Solar System objects compels us to compare subsequent thermal events recorded in eucrites to timing of bombardments to the Moon (and Earth). Morbidelli et al. (2012) argued in their "Sawtooth" model that were probably two major phases of early lunar bombardment: a primordial phase between about 4200 and 4500 Ma dominated by the leftover planetesimals of planet formation (see also Bottke et al., 2007; Walsh et al., 2011), and a second (LHB) phase induced at about 4100–4200 Ma by the later initiation of giant planet migration (e.g., Gomes et al., 2005; Bottke et al., 2012). With respect to the second phase, dynamical models that explain the current orbital architecture of the outer planets (Gomes et al., 2005; see also Nesvorný, 2011; Nesvorný and Morbidelli, 2012) contend that the impact uptick was induced by planetary migration where comets and asteroids were expelled from previously stable small body reservoirs. Such a scenario was not limited to the Earth–Moon system and by extension the LHB should be manifest in asteroid ages produced by impact heating.

Evidence for both an early bombardment phase and the LHB is present in several asteroidal meteorites and lunar meteorites. Ancient thermal events that pre-date the LBH are evident from $^{40-39}$Ar ages from eucrites and howardites and suggest they represent resetting by one or more major impact events between 4400 and 4500 Ma that may have produced the largest crater observed on Vesta (Bogard and Garrison, 2003; Bogard, 2011). This suggestion, however, would appear to be inconsistent with the revised young age of *Rheasilvia* derived by superposed crater counts from *DAWN* mission data (Marchi et al., 2012). Also, Bogard (2011) reviewed the available data of early $^{40-39}$Ar ages (i.e., before 4300 Ma), and argued that many of those ages across the stony meteorite samples analyzed to date may simply be from parent body cooling. On the other hand, the presence of impact melts and other tell-tale signs of collisions among those fragments suggests that at least some of these ages were impact generated. A U–Pb age from zircon in a lunar melt breccias and $^{40-39}$Ar ages from 2 impact-melts clasts in howardites record similar impact ages at ~4300 Ma (Cohen, 2007; Pidgeon et al., 2010).

Impacts that coincided with the proposed timing of the LHB as defined by U–Pb, K–Ar, and Rb–Sr isochrons (3800–3900 Ma) from lunar highland breccias (Tera et al., 1974) are also seen in multiple brecciated eucrites and igneous clasts in howardites which fall between 3400 and 4100 Ma (Bogard and Garrison, 2003; Bogard, 2011; Cohen, 2013). These ages appear in impact melt breccias of H-chondrites (3600–4100 Ma) and IIE irons (3700 Ma) (Bogard et al., 2000; Swindle et al., 2009, 2012). Zhou et al. (2011) proposed later thermal event age of 4195 ± 13 Ma for an apatite they measured in Béréba. These authors, presaging Morbidelli et al. (2012)

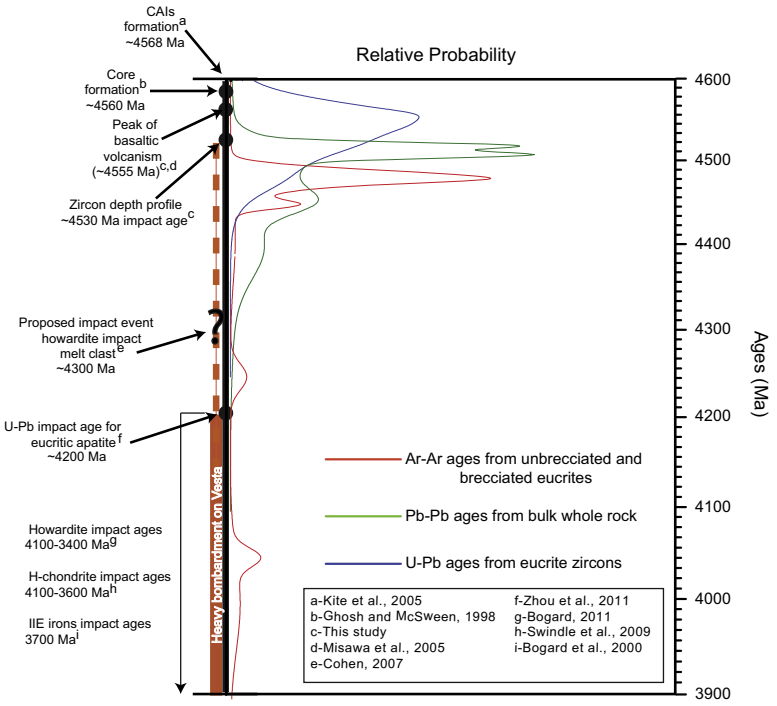

Fig. 10. Probability density curves showing the various radiometric ages of HED meteorites for the first ~150 Ma on Vesta superposed on a time-line of events. Blue curve represents U–Pb zircon ages from this study and several other studies (Ireland and Wlotzka, 1992; Bukovanská and Ireland, 1993; Bukovanská et al., 1997; Ireland and Bukovanská, 2003; Misawa et al., 2005; Zhou et al., 2013). Green curves show whole rock Pb–Pb ages from Tera et al. (1997). Red curve shows the age distribution of Ar–Ar ages for unbrecciated eucrites (Bogard and Garrison, 2003). Light gray curve shows ages from other radiometric systems including short-lived chronometers (^{146}Sm–^{142}Nd, ^{53}Mn–^{53}Cr, ^{182}Hf–^{182}W) and the long-lived ^{87}Rb–^{87}Sr chronometer (Nyquist et al., 1986, 1997; Wadhwa and Lugmair, 1995; Wadhwa et al., 2006; Trinquier et al., 2008).

suggest that the Béréba apatite age represents the start of the LHB in the asteroid belt. Several studies on zircon, baddeleyite, and apatite from lunar impact breccia samples show a range of "impact ages" from 4250 to 3900 (Pidgeon et al., 2007, 2010; Grange et al., 2009; Arai et al., 2010; Norman and Nemchin, 2014). It has also been suggested that the Moon's impact history consisted of a series of intense bombardment episodes interspersed with quite periods of relatively low impact flux rather than as a single spike at ~3900 Ma (Pidgeon et al., 2007, 2010; Grange et al., 2009). The time period 4400–4200 Ma appears to have been a quiet time on Vesta and the H chondrite parent body with relatively few impacts. Finally, Vesta meteorites apparently show no impact reset ages younger than about 3300 Ma (Swindle et al., 2009).

In light of these results, further constraints on the timing and duration of intense bombardments to the inner Solar System are required to pin down ages as an actual episode of high impact flux or simply evidence for a major impact event occurring on the Moon at that time. Continued efforts on this research front are expected to open the way to a more comprehensive picture of the impact bombardment history and tie dates to the dynamical evolution of the inner Solar System. A step in this direction is to make further use of eucrite zircons as input parameters for thermal models of Vesta's crust during bombardment (Fig. 10).

7. Conclusions

The ultra-high resolution ion microprobe depth profile technique can reveal distinct age domains within individual zircon grains previously unavailable using the conventional 2-D method. These domains provide insights into the early thermal histories of HED meteorites and show that zircon U–Pb systematics can be wholly or partially re-set even in extraterrestrial samples. We applied this technique to four zircons (>7–40 μm ∅) extracted from the brecciated eucrite Millbillillie. The continuous U–Th–Pb age profile for mb1_gr1 shows a core crystallization Pb–Pb age of 4555 ± 17 Ma, and evidence for a younger domain age of 4531 ± 20 Ma. The mb7_gr1 age profile yields a single domain Pb–Pb age of 4537 ± 18 Ma which is statistically similar to the younger age in mb1_gr1. Profiles for mb14_gr1 and mb17_gr1 show single domain Pb–Pb ages of 4520 ± 70 Ma and 4494 ± 52 Ma, respectively. Mb1_gr1 has $[Th/U]_{zrc}$ values that range from 0.8 to 1.1 and a U/Pb age profile that remains concordant throughout. These results lend support to the notion that the younger rim age was formed by recrystallization in an impact-generated melt. Although concordance remains consistent throughout sample mb7_gr1, its $[Th/U]_{zrc}$ values (0.2–0.5) suggest that later diffusion-controlled age resetting from impact shock heating is a distinct possibility. Depth profiling very small zircon grains in our sample set (mb14_gr1 and mb17_gr1) was analytically challenging, hence these data are of lower quality and overlap with all age domains present in mb1_gr1 and mb7_gr1.

Our thermal modeling predicts that an impactor with a velocity of at least 10 km s^{-1} and large enough to create the biggest known basin on Vesta, would age-reset (in zircon) ~0.2% of Vesta's volume and ~1% of its surface area. Our expectation is that large objects in a dynamically "hot" primordial asteroid belt would have had significantly higher velocities, thus enhancing the feasibility that impact-related zircons could exist on the surface. Future work that makes use of this meteoritic zircon record, and expands it to include other minerals in the same meteorite samples that have different U–Pb closure temperatures (e.g. apatite, whitlockite and sphene) will go far towards enhancing our direct understanding of the impact history of the asteroid belt.

Acknowledgments

Discussions and debates with Hal Levison, Luke Dones, Alessandro Morbidelli, Simone Marchi, Kaveh Pahlevan, Matt Wielicki,

Mark Harrison, Barb Cohen and Qing-zhu Yin have helped clarify the ideas presented here. Earlier comments by Marc Norman, Doug Mittelfeldt, Sasha Nemchin, and Trevor Ireland helped improve the manuscript. Detailed and careful reviewers from Audrey Bouvier and an anonymous reviewer are gratefully acknowledged. We thank the NASA Lunar Science Institute and the Center for Lunar Origin and Evolution (CLOE) for support. Substantial parts of this manuscript were completed while S.J.M. held a Distinguished Visiting Professorship in Budapest at the Research Center for Astronomy and Geochemistry of the Hungarian Academy of Sciences. We thank Axel Schmitt, Rita Economos and Kevin McKeegan for assistance using the Cameca ims1270 ion microprobe at UCLA. We also thank John Drexler for assistance on the CU Boulder JEOL 8200 electron microprobe, and to Blaine Reed for access to new brecciated eucrite meteorite samples.

Appendix A. Supplementary material

Supplementary data associated with this article can be found, in the online version, at http://dx.doi.org/10.1016/j.icarus.2014.08.025.

References

Abbott, S.S., Harrison, M., Mojzsis, S.J., Schmitt, A.K., 2012. A search for thermal excursions from ancient extraterrestrial impacts using Hadean zircon Ti–U–Th–Pb depth profiles. Proc. Natl. Acad. Sci. USA 109, 13486–13492.

Abramov, O., Kring, D.A., Mojzsis, S.J., 2013. The impact environment of the Hadean Earth. Chem. Erde 73, 227–248.

Ahrens, T.J., O'Keefe, J.D., 1977. Equations of state and impact-induced shock-wave attenuation on the Moon. In: Impact and Explosion Cratering. Pergamon Press, New York, pp. 639–656.

Arai, T. et al., 2010. Support for a prolonged KREEP magmatism: U–Pb age dating of zircon and baddeleyite in lunar meteorite NWA 4485. Lunar Planet. Sci. 41, 2379.

Binzel, R.P., Xu, S., 1993. Chips off of Asteroid 4 Vesta: Evidence for the parent body of basaltic achondrite meteorites. Science 260, 186–191.

Black, L.P. et al., 2003. The application of SHRIMP to Phanerozoic geochronology; a critical appraisal of four zircon standards. Chem. Geol. 200 (1–2), 171–188.

Bogard, D.D., 2011. K–Ar ages of meteorites: Clues to parent-body thermal histories. Chem. Erde 71, 207–226.

Bogard, D., Garrison, D., 2003. ^{39}Ar–^{40}Ar ages of eucrites and thermal history of Asteroid 4 Vesta. Meteorit. Planet. Sci. 38, 669–710.

Bogard, D., Garrison, D., 2009. Ar–Ar impact heating ages of eucrites and timing of the LHB. Lunar Planet. Sci. 40. Abstract #1131.

Bogard, D.D., Garrison, D.H., McCoy, T.J., 2000. Chronology and petrology of silicates from IIE iron meteorites: Evidence of a complex parent body evolution. Geochim. Cosmochim. Acta 64, 2133–2154.

Bottke, W.F., Levison, H.F., Nesvorný, D., Dones, L., 2007. Can planetesimals leftover from terrestrial planet formation produce the lunar Late Heavy Bombardment? Icarus 190, 203–223.

Bottke, W.F. et al., 2012. An Archean heavy bombardment from a destabilized extension of the asteroid belt. Nature 485, 78–81.

Britt, D.T., Macke, R.J., Kiefer, W., Consolmagno, G.J., 2010. An overview of achondrite density, porosity, and magnetic susceptibility. Lunar Planet. Sci. 41. Abstract #1869.

Bukovanská, M., Ireland, T.R., 1993. Zircons in eucrties: Pristine and disturbed U–Pb systematics. Meteoritics 28, 333.

Bukovanská, M., Ireland, T.R., Janicke, J., 1997. Zircons and baddeleyites from differentiated meteorites – Basaltic achondrites: Ion probe dating and REE systematics. Meetings of the Association of European Geological Societies 10 – Section 2.

Burbine, T.H. et al., 2001. Vesta, Vestoids and the HEDs: Relationships and the origin of spectral differences. Meteorit. Planet. Sci. 36, 761–782.

Burbine, T.H., McCoy, T.J., Meibom, A., Gladman, B., Keil, K., 2002. Meteoritic parent bodies: Their number and identification. Asteroids III, 653–667.

Carlson, R.W., Lugmair, G.W., 2000. Timescales of planetesimal formation and differentiation based on extinct and extant radioisotopes. In: Canup, R., Righter, K. (Eds.), Origin of the Earth and Moon. University of Arizona Press, Tucson, pp. 25–44.

Cates, N.L., Mojzsis, S.J., 2007. Pre-3750 Ma supracrustal rocks from the Nuvvuagittuq supracrustal belt, northern Québec. Earth Planet. Sci. Lett. 255, 9–21.

Cates, N.L., Mojzsis, S.J., 2009. Metamorphic zircon, trace elements and Neoarchean metamorphism in the ca. 3.75 Ga Nuvvuagittuq supracrustal belt, Québec (Canada). Chem. Geol. 261, 98–113.

Chamberlain, K.R., Bowring, S.A., 2000. Apatite-feldspar U–Pb thermochronometer: A reliable, mid-range (~450 °C), diffusion-controlled system. Chem. Geol. 172, 73–200.

Chapman, C.R., McKinnon, W.B., 1986. Cratering of planetary satellites. Satellites, 492–580.

Cherniak, D.J., Watson, E.B., 2001. Pb diffusion in zircon. Chem. Geol. 172, 5–24.

Cherniak, D.J., Lanford, W.A., Ryerson, F.J., 1991. Lead diffusion in apatite and zircon using ion implantation and Rutherford backscattering techniques. Geochim. Cosmochim. Acta 55, 1663–1673.

Cherniak, D.J., Watson, E.B., Grove, M., Harrison, T.M., 2004. Pb diffusion in monazite: A combined RBS/SIMS study. Geochim. Cosmochim. Acta 68, 829–840.

Cohen, B.A., 2007. Cataclysmic bombardment recorded in ^{40}Ar–^{39}Ar ages of impact melt clasts in howardites. 70th Annual Meteoritical Society Meeting, 5212.

Cohen, B.A., 2013. The Vestal Cataclysm: Impact-melt clasts in howardites and the bombardment history of 4 Vesta. Meteorit. Planet. Sci. 48, 771–785.

Collins, G.S., Melosh, H.J., Morgan, J.V., Warner, M.R., 2002. Hydrocode simulations of Chicxulub crater collapse and peak-ring formation. Icarus 157, 24–33.

Croft, S.K., 1985. The scaling of complex craters. J. Geophys. Res. 90, 828–842.

Dauphas, N., Pourmand, A., 2011. Hf–W–Th evidence for rapid growth of Mars and its status as a planetary embryo. Nature 473, 489–492.

Davies, G.F., 1972. Equations of state and phase equilibria of stishovite and coesite-like phase from shock-wave and other data. J. Geophys. Res. 77, 4920–4933.

Dodson, M.H., 1973. Closure temperature in cooling geochronological and petrological systems. Contrib. Mineral. Petrol. 40, 259–274.

Ghosh, A., McSween, H.Y. Jr., 1998. A thermal model for the differentiation of asteroid 4 Vesta, based on radiogenic heating. Icarus 134, 187–206.

Gilbert, G.K., 1893. The Moon's face. Bull. Philos. Soc. Washington 12, 241–292.

Gomes, R., Levison, H.F., Tsiganis, K., Morbidelli, A., 2005. Origin of the cataclysmic Late Heavy Bombardment period of the terrestrial planets. Nature 435, 466–469.

Grange, M.L., Nemchim, A.A., Pidgeon, R.T., Timms, N., Muhling, J., Kennedy, A., 2009. Thermal history recorded by the Apollo 17 impact melt breccia 73217. Geochim. Cosmochim. Acta 73, 3093–3107.

Greenwood, R.C., Franchi, I.A., Jambon, A., Barrat, J.A., Burbine, T.H., 2005. Oxygen isotope variation in stony-iron meteorites. Science 313, 1763–1765.

Hartmann, W.K., Ryder, G., Dones, L., Grinspoon, D., 2000. The time-dependent intense bombardment of the primordial Earth/Moon system. In: Canup, R., Righter, K. (Eds.), Origin of the Earth and Moon. University of Arizona Press, Tucson, pp. 493–512.

Heaman, L.M., LeCheminant, A.N., 1993. Paragenesis and U–Pb systematics of baddeleyite (ZrO_2). Chem. Geol. 110, 95–126.

Heaman, L.M., Lecheminant, A.N., 2000. Anomalous U–Pb systematics in mantle-derived baddeleyite xenocrysts from le Bizard: Evidence for high temperature radon diffusion? Chem. Geol. 172, 77–93.

Heisinger, H., Head, J.W., 2006. New views of lunar geoscience: An introduction and overview. In: Jolliff, B.L., Wieczorek, M.A., Shearer, C.K., Neal, C.R. (Eds.), New Views of the Moon. Reviews in Mineralogy and Geochemistry, vol. 60, pp. 1–81.

Herzberg, C., 1995. Phase equilibria of common rocks in the crust and mantle. In: Ahrens, T.J. (Ed.), Rocks Physics & Phase Relations: A Handbook of Physical Constants. AGU Reference Shelf, vol. 3, pp. 166–177.

Hoskin, P.W.O., Schaltegger, U., 2003. The composition of zircon and igneous and metamorphic petrogenesis. Rev. Mineral. Geochem. 53, 27–62.

Ireland, T.R., Bukovanská, M., 2003. Initial ^{182}Hf/^{180}Hf in meteoritic zircons. Geochim. Cosmochim. Acta 67, 4849–4856.

Ireland, T.R., Wlotzka, F., 1992. The oldest zircons in the Solar System. Earth Planet. Sci. Lett. 190, 1–10.

Keil, K., 2000. Geological history of Asteroid 4 Vesta: The "smallest terrestrial planet". Asteroids III 1807, 573–584.

Kieffer, S.W., Simonds, C.H., 1980. The role of volatiles and lithology in the impact cratering process. Rev. Geophys. Space Phys. 18, 143–181.

Kita, N.T., Huss, G.R., Tachibana, S., Amelin, Y., Nyquist, L.E., Hutcheon, I.D., 2005. Constraints on the origin of chondrules and CAIs from short-lived and long-lived radionuclides. In: Krot, A.N., Scott, E.R.D., Reipurth, B. (Eds.), Chondrites and the Protoplanetary Disk. Astron. Soc. Pacific Conf. Ser. 341, pp. 558–587.

Kleine, T., Mezger, K., Palme, H., Scherer, E., Münker, C., 2004. The W isotope composition of the thermal metamorphism of basaltic eucrites. Earth Planet. Sci. Lett. 231, 41–52.

Kleine, T. et al., 2009. Hf–W chronology of the accretion and early evolution of asteroids and terrestrial planets. Geochim. Cosmochim. Acta 73, 5150–5188.

Leyrat, C., Barucci, A., Mueller, T., O'Rourke, L., Valtchanov, I., Fornasier, S., 2012. Thermal properties of (4) Vesta derived from Herschel measurements. Annu. Rev. Astron. Astrophys. 539, A154.

Ludwig, K.R., 2003. User's manual for Isoplot/Ex: A geochronological toolkit for Microsoft Excel. Berkley Geochronological Cent. Spec. Publ., 4.

Lugmair, G.W., Shukolyukov, A., 1998. Early Solar System timescales according to ^{53}Mn–^{53}Cr systematics. Geochim. Cosmochim. Acta. 62, 2863–2886.

Marchi, S. et al., 2012. The violent collisional history of Asteroid 4 Vesta. Science 336, 690–694.

Marchi, S., Bottke, W.F., Cohen, B.A., Wünnemann, K., Kring, D.A., McSween, H.Y., DeSanctis, M.C., O'Brien, D.P., Schenk, P., Raymond, C.A., Russell, C.T., 2013. High-velocity collissions from the lunar cataclysm recorded in asteroidal meteorites. Nat. Geosci. 6, 303–307.

McCord, T.B., Adams, J.B., Johnson, T.V., 1970. Asteroid Vesta: Spectral reflectivity and compositional implications. Science 168, 1445–1447.

McCoy, T.J., Beck, A., McSween Jr., H.Y., and DAWN Team, 2012. Dawn, Vesta and the Hed's: The expected, the explained, and the surprises. 75th Annual Meteoritical Society Meeting. Abstract #5319.
McSween, H.Y., Mittlefehldt, D.W., Beck, A.W., Mayne, R.G., McCoy, T.J., 2011. HED meteorites and their relationship to the geology of Vesta and the Dawn mission. Space Sci. Rev. 163, 141–174.
Minton, D.A., Malhotra, R., 2009. A record of planet migration in the main asteroid belt. Nature 457, 1109–1111.
Minton, D.A., Malhotra, R., 2011. Secular resonance sweeping of the main asteroid belt during planet migration. Astrophys. J. 732, 53(1–12).
Misawa, K., Yamaguchi, A., Kaiden, H., 2005. U–Pb and ^{207}Pb–^{206}Pb ages of zircons from basaltic eucrites: Implications for early basaltic volcanism on the eucrite parent body. Geochim. Cosmochim. Acta 69, 5847–5861.
Mittlefehldt, D.W., McCoy, T.J., Goodrich, C.A., Kracher, A., 1998. Non-chondritic meteorites from asteroidal bodies. In: Papike, J.J. (Ed.), Planetary Materials, Reviews in Mineralogy, vol. 3. Mineral. Soc. Am., Washington, p. 195.
Miura, Y., Nagao, K., Sugiura, N., Fujitani, T., Warren, P., 1998. Noble gases, ^{81}Kr–Kr exposure ages and ^{244}Pu–Xe ages of six eucrites, Bereba, Binda, Camel Donga, Juvinas, Millbillillie, and Stannern. Geochim. Cosmochim. Acta 62, 2369–2387.
Mojzsis, S.J., Harrison, T.M., 2002. Establishment of a 3.83-Ga magmatic age for the Akilia tonalite (southern West Greenland). Earth Planet. Sci. Lett. 202, 563–576.
Mold, P., Bull, R.K., Durrani, S.A., 1984. Fission-track annealing characteristic of meteoritic phosphates. Nucl. Tracks 9, 119–128.
Morbidelli, A., Marchi, S., Bottke, W.F., Kring, D.A., 2012. A sawtooth-like timeline for the first billion years of lunar bombardment. Earth Planet. Sci. Lett. 355–356, 144–151.
Müller, T.G., Lagerros, J.S.V., 2003. Asteroids as calibration standards in the thermal infrared – Applications and results from ISO. In: Metcalfe, L., Salama, A., Peschke, S.B., Kessler, M.F. (Eds.), The Calibration Legacy of the ISO Mission. ESA SP 481. ESA Publication Division, Noordwijk, pp. 157–163.
Nesvorný, D., 2011. Young Solar System's fifth giant planet. Astrophys. J. 742, L22.
Nesvorný, D., Morbidelli, A., 2012. Statistical study of the early Solar System's instability with four, five, and six giant planets. Astron. J. 144, 117.
Norman, M.D., Nemchin, A.A., 2014. A 4.2 billion year old impact basin on the Moon: U–Pb dating of zirconolite and apatite in lunar melt rock 67955. Earth Planet. Sci. Lett. 388, 387–398.
Nyquist, L.E., Takeda, H., Bansal, B.M., Shih, C.-Y., Wiesmann, H., Wooden, J.L., 1986. Rb–Sr and Sm–Nd internal isochron ages of a subophitic basalt clast and matrix sample from the Y75011 eucrite. J. Geophys. Res. 91, 8137–8150.
Nyquist, L.E., Bogard, D., Takeda, H., Bansal, B., Wiesmann, H., Shih, C.-Y., 1997. Crystallization, recrystallization, and impact-metamorphic ages of eucrites Y792510 and Y791186. Geochim. Cosmochim. Acta 61, 2119–2138.
Nyquist, L.E., Reese, Y., Wiesmann, H., Shih, C.-Y., Takeda, H., 2001a. Dating eucrite formation and metamorphism (abstract). Antarct. Meteorit. XXVI, 113–115.
Nyquist, L.E., Bogard, D.D., Shih, C.-Y., Greshake, A., Stoffler, D., Eugster, O., 2001b. Ages and geological histories of martian meteorites. Chronol. Evol. Mars, 105–164.
Nyquist, L.E., Shih, C.Y., Reese, Y.D., 2008. Sm–Nd for norite 78236 and eucrite Y980318/433: Implications for planetary and Solar System processes. Lunar Planet. Sci. XXXIX, 1437.
Paces, J.B., Miller Jr., J.D., 1993. Precise U–Pb ages of Duluth Complex and related mafic intrusions, northeastern Minnesota; geochronological insights to physical, petrogenetic, paleomagnetic, and tectonomagnetic processes associated with the 1.1 Ga Midcontinent Rift System. J. Geophys. Res. 98, 13997–14013.
Papike, J.J., Karner, J.M., Shearer, C.K., 2003. Determination of planetary basalt parentage: A simple technique using the electron microprobe. Am. Mineral. 88, 469–472.
Pidgeon, R.T. et al., 2007. Complex history of a zircon aggregate from lunar breccia 73235. Geochim. Cosmochim. Acta 71, 1370–1381.
Pidgeon, R.T., Nemchin, A.A., Grange, M.L., Meyer, C., 2010. Evidence for a lunar ''cataclysm'' at 4.34 Ga from zircon U–Pb systems. Lunar Planet. Sci. 41. Abstract #1126.
Pierazzo, E., Melosh, H.J., 2000. Melt production in oblique impacts. Icarus 145, 252–261.
Pierazzo, E., Vickery, A.M., Melosh, H.J., 1997. A reevaluation of impact melt production. Icarus 127, 408–423.
Rubin, A., 1997. Mineralogy of meteorite groups. Meteorit. Planet. Sci. 32, 231–247.
Russell, C.T. et al., 2012. Dawn at Vesta: Testing the protoplanetary paradigm. Science 336, 684–686.
Ryder, G., 2002. Mass flux in the ancient Earth–Moon system and benign implication for the origin of life on Earth. J. Geophys. Res. 107 (E4), 5002.
Sano, Y., Terada, K., Takeno, S., Taylor, L.A., Mcsween, H., 2000. Ion microprobe uranium–thorium–lead dating of Shergotty phosphates. Meteorit. Planet. Sci. 35, 341–346.
Schmidt, R.M., Housen, K.R., 1987. Some recent advances in the scaling of impact and explosion cratering. Int. J. Impact Eng. 5, 543.
Schmitz, M.D., Bowring, S.A., Ireland, T.R., 2003. Evaluation of Duluth Complex anorthositic series (AS3) zircon as a U–Pb geochronological standard: New high precision isotope dilution thermal ionization mass spectrometry results. Geochim. Cosmochim. Acta 67, 3665–3672.
Shoemaker, E.M., 1962. Interpretation of lunar craters. In: Kopal, Z. (Ed.), Physics and Astronomy of the Moon. Academic Press, San Diego, pp. 283–359.
Shukolyukov, A., Begemann, F., 1996. Cosmogenic and fissiogenic noble gases and ^{81}Kr–Kr exposure age clusters of eucrites. Meteorit. Planet. Sci. 31, 60–72.
Srinivasan, G., Goswami, J.N., Bhandari, N., 1999. ^{26}Al in eucrite Piplia Kalan: Plausible heat source and formation chronology. Science 284, 1348–1350.
Srinivasan, G., Whitehouse, M.J., Weber, I., Yamaguchi, a., 2007. The crystallization age of eucrite zircon. Science 317, 345–347.
Stöffler, D., Ryder, G., 2001. Stratigraphy and isotope ages of lunar geologic units: Chronological standards for the inner Solar System. Space Sci. Rev., 9–54.
Swindle, T.D., Isachsen, C.E., Weirich, J.R., Kring, D.A., 2009. ^{40}Ar–^{39}Ar ages of H chondrite impact melt breccias. Meteorit. Planet. Sci. 44, 747–762.
Swindle, T.D., Kring, D.A., Wierich, J.R., 2012. ^{40}Ar–^{39}Ar ages of impacts involving ordinary chondrite meteorites. In: ^{40}Ar/^{39}Ar Dating: From Geochronology to Thermochronology, from Archeaology to Planetary Science. Geological Society, London, Special Publications 378 (2013).
Tang, H., Dauphas, N., 2012. Abundance, distribution, and origin of ^{60}Fe in the solar protoplanetary disk. Earth Planet. Sci. Lett. 359–360, 248–263.
Tera, F., Papanastassiou, D.A., Wasserburg, G.J., 1974. Isotopic evidence for a terminal lunar cataclysm. Earth Planet. Sci. Lett. 22, 1–21.
Tera, F., Carlson, R.W., Boctor, N.Z., 1997. Radiometric ages of basaltic achondrites and their relation to the early history of the Solar System. Geochim. Cosmochim. Acta 61, 1713–1731.
Trail, D., Mojzsis, S.J., Harrison, T.M., 2007. Thermal events documented in Hadean zircons by ion microprobe depth profiles. Geochim. Cosmochim. Acta 71, 4044–4065.
Trinquier, A., Birck, J.L., Allègre, C.J., Gopel, C., Ulfbeck, D., 2008. ^{53}Mn–^{53}Cr systematics of the early Solar System revisited. Geochim. Cosmochim. Acta 72, 5146–5163.
Vilas, F., Cochran, A.L., Jarvis, K.S., 2000. Vesta and the Vestoids: A new rock group? Icarus 147, 119–128.
Wadhwa, M., Lugmair, G.W., 1995. Sm–Nd systematics of the eucrite Chervony Kut. Lunar Planet. Sci. XXVI, 1453–1454.
Wadhwa, M., Lugmair, G.W., 1996. Age of the eucrite "Caldera" from the convergence of long-lived and short-lived chronometers. Geochim. Cosmochim. Acta 60, 4889–4893.
Wadhwa, M., Srinivasan, G., Carlson, R.W., 2006. Timescales of planetesimal differentiation in the early Solar System. In: Lauretta, D.S., Mc Sween, H.Y., Jr. (Eds.), Meteorites and the Early Solar System II. University of Arizona Press, Tucson, pp. 715–731.
Walsh, K.J., Morbidelli, A., Raymond, S.N., O'Brien, D.P., Mandell, A.M., 2011. A low mass for Mars from Jupiter's early gas-driven migration. Nature 475, 206–209.
Watson, E.B., Harrison, T.M., 2005. Zircon thermometer reveals minimum melting conditions on earliest Earth. Science 308, 841–844.
Wiechert, U.H., Halliday, A., Palme, H., Rumble, D., 2004. Oxygen isotope evidence for rapid mixing of the HED meteorite parent body. Earth Planet. Sci. Lett. 221, 373–382.
Wiedenbeck, M. et al., 2004. Further characterization of the 91500 zircon crystal. Geostand. Geoanal. Res. 28, 9–39.
Zahnle, K., Schenk, P., Levison, H., Dones, L., 2003. Cratering rates in the outer Solar System. Icarus 163, 263–289.
Zhou, Q. et al., 2011. Early basaltic volcanism and Late Heavy Bombardment on Vesta: U–Pb ages of small zircons and phosphates in eucrites. Lunar Planet. Sci. 42. Abstract #2575.
Zhou, Q. et al., 2013. SIMS Pb–Pb and U–Pb age determination of eucrite zircons at <5 micron scale and the first 50 Ma of the thermal history of Vesta. Geochim. Cosmochim. Acta 110, 152–175.